

Clastrum: a case for directional, excitatory, intrinsic connectivity in the rat

Rena Orman¹

Received: 22 July 2015 / Accepted: 16 August 2015 / Published online: 2 September 2015
© The Physiological Society of Japan and Springer Japan 2015

Abstract Clastrum, a gray matter structure that underlies the neocortex, is reciprocally connected with many neocortical and limbic cortical areas. This connectivity positions claustrum ideally for the integration or coordination of widespread cortical activity. In anatomical studies using multiple planes of section, claustrum has distinct subregions based on latexin immunohistochemistry, and an approximately rostro-caudal alignment of fusiform cells supporting a laminar intrinsic organization. Physiological studies of claustral connectivity in disinhibited brain slices demonstrate (1) intrinsic connectivity sufficient to generate spontaneous synchronized burst discharges, (2) activity spread within the oblique laminae that contained the principal cellular axis, and (3) segregation of activity as evidenced by the absence of spread within coronal planes. Activity spread depended on glutamatergic synaptic transmission, and activity restrictions did not depend on inhibitory circuits. We conclude that the claustrum has an intrinsic excitatory connectivity that is constrained in approximately rostro-caudal laminae, with minimal cross-communication between laminae. Further, claustrum has the intrinsic capability of generating synchronized population activity and facilitating its spread within laminae, a feature that may contribute to seizure generation and spread.

Keywords Clastrum · Glutamate · Excitatory synapse · Epilepsy

Introduction

Clastrum is a sheet-like subcortical region that is literally sandwiched between the external and extreme capsules in primate brains, and located just beneath the neocortex (above the external capsule) in lower mammalian brains ([1]; for reviews: [2–6]). Anatomical data show cortico-claustral and claustral-cortical circuits involving most sensory neocortical regions. Clastrum has reciprocal projections to a large number of cortical areas, including visual [7–12], motor [9, 11, 13–16], somatosensory [9, 11, 14, 15, 17], auditory [11, 14, 17, 18], olfactory [13, 19], gustatory [19], prefrontal [20], and limbic cortices [13, 21–25]. In general, the part of claustrum projecting to a cortical region is larger than the part of claustrum receiving inputs from that region [26].

There are “zones” of claustrum associated with particular cortical regions. Most notably, somatosensory cortices are associated with the dorsal-most parts of claustrum, with cells running in a largely horizontal stripe through the structure. Auditory and visual cortices are associated with a claustral zone that is ventral to the zone for the somatosensory cortex [11, 27–33]. Claustral neurons in distinct zones, while having large receptive fields, were responsive to particular sensory modalities (visual, somatosensory, or auditory) [27]. Largely as a result of its rich reciprocal connectivity with the neocortex, functional speculation has been dominated by the notion that claustrum is perfectly positioned to coordinate activity in widely separated cortical areas associated with different sensory modalities [34, 35] (see also reviews above).

✉ Rena Orman
rena.orman@downstate.edu

¹ Department of Physiology and Pharmacology, State University of New York Downstate Medical Center, 450 Clarkson Avenue, MSC 31, Brooklyn, NY 11203, USA

A majority of the claustrum-cortical projection is excitatory. Asymmetrical claustrum-cortical synapses consistent with excitatory synapses have been seen in electron micrographs [10]. Some of the claustrum-cortical projection was shown using tritiated-aspartate labeling to be an excitatory glutamatergic projection [36], but not all of it. A portion of the projection to visual cortex was found to be non-glutamatergic (projection cells stained for nitric oxide), but this was still considered to be an excitatory projection because 24/29 visual cortical cells decreased their firing when nitric oxide (NO) was inhibited [37]. The inhibitor used by these investigators, L-NG-nitro arginine, is effective against constitutive (neuronal) nitric oxide synthase (NOS), but also against endothelial and inducible forms.

Some of the claustral outflow is also inhibitory. Large aspiny cells are known to be projection cells [38], and a fraction of visual cortical neurons (4/29) increased their firing when NO was inhibited, suggesting an inhibitory NOS-positive projection from claustrum [37]. A number of claustral NOS-positive cells were shown to be inhibitory neurons [39]. From a functional standpoint, a number of details of the cellular targets of the claustrum-cortical projection remain unknown (i.e., a glutamatergic projection may be functionally inhibitory by terminating on inhibitory cortical neurons; shown in [10]).

On the basis of Golgi staining or retrograde tracer labeling, there are basically three cell types based on dendritic spininess (medium-sized spiny, medium-sized aspiny, and small aspiny cells) and on whether cells have projection axons that could be identified to leave claustrum [38, 40, 41]. Each of these groups can be subdivided or sorted into alternative groups based on soma shape, patterns of dendritic branching, or immunocytochemistry (e.g., [42, 43]). It has been estimated that about 12 % of claustral neurons are GABAergic [44, 45]. These have been subdivided on the basis of immunocytochemistry for parvalbumin, calbindin, calretinin, NOS activity, and assorted peptides (e.g., [43, 45–49]).

The intrinsic organization of claustral neurons has been more difficult to study because of the challenges imposed by its curved, slender shape. In preliminary studies, we discovered in rats that the dendrites of many claustral cells were aligned in an oblique plane off the horizontal, parallel to the rhinal fissure. This suggested that an oblique plane of section would preserve the whole claustral cell structure and permit a more complete examination of intrinsic claustral connectivity. We used latexin immunohistochemistry [50, 51] to stain claustral cells and tested different brain slice planes in studies of claustral cell connectivity. Preliminary versions of these data have been presented previously [52, 53].

Methods

Anatomical methods

Animals, sectioning

Male Sprague–Dawley albino rats (4–5 weeks old) were anesthetized with halothane or isoflurane and perfused transcardially with phosphate-buffered saline (PBS) followed by 4 % paraformaldehyde in PBS. Brains were removed, post-fixed for 18 h at 4° C in 4 % paraformaldehyde in PBS, and transferred to 30 % sucrose for cryoprotection. Frozen sections were cut at 40 µm thickness in coronal, horizontal, and oblique planes. The optimal oblique plane orientation for capturing claustral cell dendrites (see “Results”) was tilted anterior-up by 30° off the horizontal to be parallel with the rhinal fissure.

Immunohistochemistry

Adjacent sections were stained with latexin antibodies (gift by Dr. Y. Arimatsu to R. Orman) and NeuN antibodies (EMD Millipore, Temecula, CA, USA). In each case, sections were blocked for 2 h in normal serum of animals in which the secondary antibodies were raised, exposed overnight to primary antibodies at 4° C, incubated with 1 % H₂O₂ for 20 min, incubated with secondary antibodies (Vector biotinylated secondary antibodies; Vector Laboratories, Burlingame, CA, USA) for 1 h at room temperature, incubated in ABC reagents (Vector) for 30 min, and finally incubated in a peroxide substrate DAB kit (Vector). Protocol details, including standard reagents, were followed according to published kit descriptions from Vector Laboratories or general immunohistochemistry protocols from Abcam (Cambridge, MA, USA; <http://www.abcam.com/protocols/immunostaining-paraffin-frozen-free-floating-protocol>) and IHC World (Ellicott City, MD, USA; http://www.ihcworld.com/general_IHC.htm). After developing, sections were mounted on tissue-tack slides (Polyscience, Niles, IL, USA), air-dried, dehydrated, and cover-slipped.

Microscopy

Slides were viewed and photographed using (1) a plan-apochromatic stereomicroscope (M80; Leica, Bannockburn, IL, USA) with high-resolution digital camera (Leica IC80 HD; Leica; full-screen image capture 2048 × 1536 pixels, 3.1 megapixels; courtesy of Dr. Richard Kollmar) and/or (2) an upright compound microscope (Jenaval; Carl Zeiss) with motorized stage and focus control, full set of objectives, high resolution camera (1600 × 1200;

Optronics Microfire; Optronics, Goleta, GA, USA), and software (NeuroLucida 10; MBF Bioscience, Williston, VT, USA).

Brain slice physiology

Slice preparation and multi-electrode recordings

Male Sprague–Dawley albino rats (3–5 weeks old) were anesthetized with halothane or isoflurane and decapitated. Each brain was removed from the skull, bisected, and placed briefly in ice-cold artificial CSF. Thick slices of tissue (about 1–2 mm thick) were cut from intact hemispheres in planes of section that were horizontal, coronal, sagittal, or angled plane in between coronal and horizontal. Thin slices (380 μm) were cut using a motorized sectioning system (Leica VT1000S, Leica Biosystems, Buffalo Grove, IL, USA) and transferred to a holding chamber.

From the holding chamber, single slices were placed in the MED64 chamber (Panasonic MED64, Osaka, Japan). The MED64 chamber allows simultaneous extracellular recordings from 64 electrodes (50 μm squares). Each electrode is a platinum black-plated square embedded in the floor of the recording chamber. Inter-electrode distances (center to center) were 150, 300, or 450 μm . Recording electrode impedances are 22 k Ω (at 1 kHz) and each is referred to a single set of 4 reference electrodes in the periphery of the chamber that are electrically tied together. The recording electrodes are arranged in an 8 \times 8 array embedded on the bottom of the chamber. The temperature of the MED64 chamber was maintained at 30 $^{\circ}\text{C}$ by warming the perfusate with an inline heater (TC-324B; Warner Instrument, Hamden, CT, USA).

The perfusion solution (1 ml/min) was composed of (in mM): NaCl 125, KCl 2.5–5, CaCl₂ 1.7, MgCl₂ 1.2, NaHCO₃ 26, and glucose 10; pH = 7.4 when exposed to 95 % O₂/5 % CO₂.

Brief stimulating pulses were delivered using platinum-iridium parallel bipolar stimulating electrodes (150 μm tip separation; FHC, Bowdoinham, ME, USA) with <100 k Ω electrode impedances. Stimuli were biphasic pulses (50–100 μs in total duration) applied through constant current stimulus isolation units. The bipolar stimulating electrode was placed from the top side of the slice.

Data were digitized at 20 kHz per channel and stored on disk using MED64 Conductor software. Events were studied offline using MED64 Conductor software or custom Microsoft EXCEL macros.

Pharmacology

All drugs were applied to the bath by adding them to the perfusate reservoir. The concentrations given are

concentrations that exist in the reservoir and were achieved in the recording chamber over a period of minutes. Recordings in the presence of all drugs were taken after sufficient time for equilibration in the recording chamber. Equilibration was apparent in recordings as a stable change in evoked responses.

Bicuculline (bicuculline methiodide, 50 μM), AP-5 (DL-(-)-2-amino-5-phosphonopentanoic acid, 40 μM), CPP (3-((RS)-2-carboxypiperazin-4-yl)-propyl-1-phosphonic acid, 20 μM), and CNQX (6-cyano-7-nitroquinoxaline-2,3-dione or 6-cyano-7-nitroquinoxaline-2,3-dione disodium, 20 μM) and all other chemicals, unless otherwise specified, were obtained from Sigma (Sigma-Aldrich, St. Louis, MO, USA). Some batches of CNQX and CPP were obtained from Tocris Bioscience (Ellisville, MO, USA). Bicuculline was used to antagonize GABA-A receptors. AP5 and CPP were used as NMDA receptor antagonists, and CNQX was used as an AMPA receptor antagonist. All slices were disinhibited with bicuculline.

Slice planes

Three different planes of section were studied in detail. The first plane of section was a standard coronal section. This plane captures dorsal claustrum, endopiriform nucleus (ventral claustrum), and the transitional region between them. The second plane is a standard sagittal section. Some slices cut for physiology will contain dorsal and ventral claustrum in a single slice. The third plane of section is referred to as “oblique.” This slice is an angled horizontal slice where the rostral end is elevated above the caudal end, parallel to the rhinal fissure. A relatively small number of conventional horizontal slices were also tested, but these slices resembled coronal slices in activity spread and were not studied further.

Statistics

Calculations of frequency distributions, ANOVA, multiple comparisons, Fisher exact tests, and descriptive statistics were done with Microsoft Excel, IBM SPSS Statistics (v.21), and GraphPad Prism 6 software or online calculators at graphpad.com.

Results

Anatomical findings

Latexin immunohistochemistry and regional definitions

As reported by Arimatsu et al. [51, 54–56], latexin is expressed in cortical and claustral neurons. Adjacent

sections were stained for latexin and NeuN. NeuN is widely used as a cell stain in brain sections and was used here for orientation purposes and relationship of our planes of section to planes of section published elsewhere in the original literature and brain atlases. Based on our latexin staining in multiple planes of section (Fig. 1), we identified three parts of dorsal (insular) claustrum and two parts of the endopiriform nucleus [57]. In coronal sections, latexin-positive neurons and neuropil form the lateral aspect of either region. The latexin-positive region of endopiriform nucleus forms a crescent-shaped shell to a latexin-negative medial core. In the claustrum, the latexin-positive region laterally borders a small dorsal latexin-negative zone and a larger, very densely-stained latexin-positive zone located between the claustral and endopiriform latexin-negative regions (Figs. 1, 2). This very densely-stained, latexin-positive, “egg-shaped” zone is the major part of claustrum that specifically overlaps with every anatomical definition of boundaries, including the major brain atlases, e.g., [58], G-protein gamma 2 subunit (Gng2) staining [4, 59], and N- and R-cadherin staining [47].

In staining coronal, horizontal, and sagittal series, we determined that an oblique plane of section whose long axis tilted upward on the rostral end, parallel to the rhinal fissure, was optimal for preserving the predominantly bipolar, latexin-positive claustral cells. Their main dendritic shafts extended both anterodorsally and postventrally parallel to an obliquely oriented long axis of the insular claustrum (Fig. 2a). By contrast, in coronal sections, the stained claustral neurons of the principal egg-shaped zone appear as larger circular cross-sections that are set in a dense neuropil and interspersed among densely-stained smaller cross-sections of claustral cell dendrites (Fig. 2b). These findings clearly suggest a laminar organization to claustral cells that runs along the long axis of the structure.

Physiological findings

Synchronous population activity in disinhibited slices

To focus on the excitatory connectivity within claustrum, recordings of spontaneous and evoked activity were taken in the presence of GABA receptor blockade (bicuculline 50 μM unless otherwise indicated). Synchronous population events consisting of an initial population spike followed by multiple secondary population spikes were obtained in claustral recordings (Figs. 3, 4, 6 with specific features described in detail below). Claustral events evoked or triggered by single stimulus pulses applied to the overlying neocortex were identical in population spike morphology and spatial distribution to spontaneous claustral

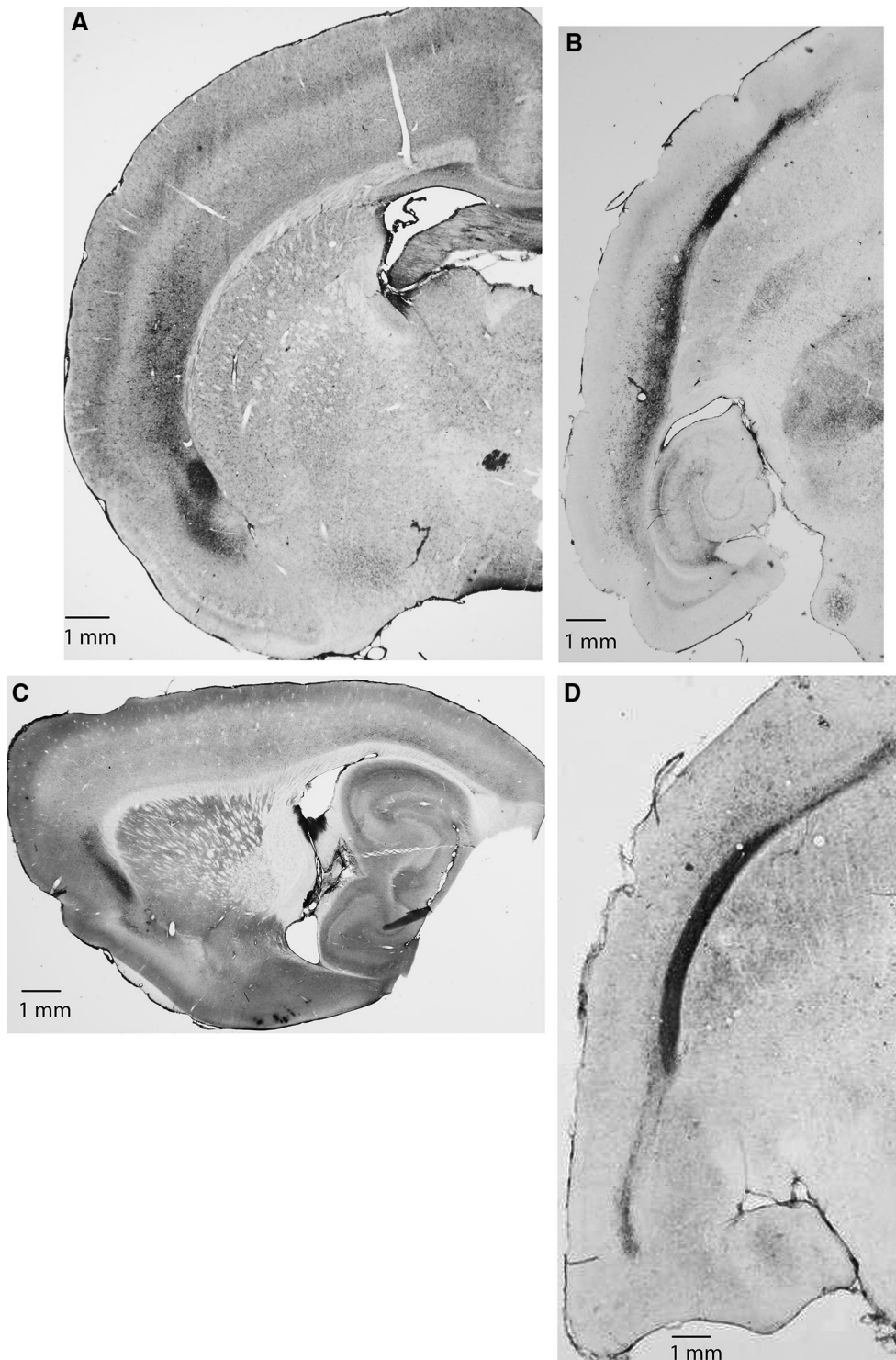
Fig. 1 Latexin staining of the rat claustrum in four planes of section. **a** Coronal section at a plane approximately 1 mm caudal to bregma [57, 58]. The densely latexin-stained, “egg-shaped,” principal subregion of claustrum is located in the same horizontal plane as the rhinal fissure. The latexin-negative medial core of endopiriform nucleus and its crescent-shaped latexin-positive shell are visible ventral to the densely-stained “egg-shaped” region of claustrum. A latexin-positive, but less densely-stained group of cells extend dorsally and border a latexin-negative region located medially. These two subregions are also debatably part of claustrum, but our study concentrates on the “egg-shaped” subregion that appears in every definition of claustrum. **b** Horizontal section at a plane approximately 6.6 mm below bregma. The principal claustral subregion is evident at about 1/3 of the distance from the *top* of the figure, but sparser staining rostrally (endopiriform nucleus and caudally (claustral cells dorsal to the densest staining) are evident. **c** Sagittal section at a plane approximately 4.6 mm lateral to the midline highlights the densely-stained claustrum. **d** An oblique section that optimizes capture of latexin-positive claustral cell dendrites. This section was cut at 30° off the horizontal in a rostro-dorsal to caudo-ventral direction. *Scale bars* 1 mm

events identified as claustral in origin by the identification of the first site in the slice showing activity.

Spatial extent of activity spread within claustrum

One of the most dramatic findings was that the oblique slice plane captured synchronous population activity on the largest number of electrodes. As a measure of the extent of synchronous activity spread, we determined the number of electrode channels in claustrum with synchronous spiking divided by the total number of electrode channels in claustrum for each slice. Oblique slices captured larger amounts of claustral tissue and therefore had the largest number of electrode channels in claustrum (an average of 11 electrodes in claustrum depending on grid spacing compared with an average of 5 electrodes for coronal and sagittal slices; see Figs. 3, 4). In 16/33 oblique slices, every electrode in claustrum showed synchronous population activity (Fig. 3). Coronal slices were at the other extreme, with 62 of 65 slices showing activity on 0 or 1 electrode (Fig. 4). Sagittal slices were inbetween, showing statistically larger fractions than coronal slices, but statistically smaller fractions than oblique slices. The mean fractions (\pm SEM) for each group were: coronal 5.5 ± 1.8 , oblique 63 ± 6.9 , and sagittal 28 ± 7.5 % of claustral electrodes showing synchronous spiking. Median fractions were 0, 75, and 20 for coronal, oblique, and sagittal slices, and the 75th percentile was 0, 100, and 50 for the three groups. These data are summarized in Fig. 5.

An ANOVA showed the differences for the dataset to be highly significant ($F_{2,114} = 49.81$; $p < 0.0001$) as well as the multiple comparisons (corlsag, $p = 0.0021$; corlobl, $p < 0.0001$; saglobl, $p < 0.0001$; Holm-Sidak’s multiple comparisons tests). Comparing the groups based on the



presence of synchronous spiking on ≤ 1 electrode or > 1 electrode, the distributions were all statistically different from each other: coronal 62, 3, oblique 8, 25, and sagittal 12, 7 (two-tailed Fisher exact tests: corlsag, $p = 0.0009$; corobl, $p < 0.0001$; sagobl, $p = 0.0081$).

We note that the statistical significance is underestimated because our calculations of fractional involvement are

extremely conservative. The numbers of electrodes in claustrum in coronal and sagittal slices were smaller, averaging 5 electrodes in claustrum (ranges: 2–11 coronal, 3–7 sagittal), compared with oblique slices, which averaged 11 electrodes in claustrum (range: 4–16). This caused higher fractions with fewer electrodes in coronal and sagittal slices, and lower fractions with more electrodes in the oblique

slices. The average number of electrodes in claustrum for each of the three planes of section was: coronal 5 (range 2–11), oblique 11 (range 4–16), and sagittal 5 (range 3–7).

Given the overall shape of claustrum, i.e., a thin sheet-like structure whose thinnest dimension is along the mediolateral axis, sagittal slices are the most likely to be variable with regard to the amount of claustral tissue captured in a slice. We believe this accounts for the intermediate level of fractional activity in the slices. Whereas oblique slices capture both the principal dendritic axis of claustral cells and long stretches of claustral tissue over multiple sections, sagittal slices capture the dendritic axis, but only offer one or two slices per hemisphere with adequate claustral tissue to study intrinsic connectivity. Coronal slices cut the dendritic axes nearly perpendicularly, and, although many sections contain claustral tissue, intrinsic connectivity is largely abolished.

Spread rate and directional constraints within claustrum

A hallmark of cell-to-cell connectivity among excitatory cells is the generation spontaneous population bursts when inhibitory synaptic transmission is blocked, and the spread of these events over distances within the structure. As described above, synchronous population events that spread over large distances in claustrum were seen in the oblique slices, less commonly in the sagittal slices, and essentially not at all in the coronal slices. In oblique slices that captured long lengths of the densely latexin-positive staining, the spread rate for spontaneous or evoked population events was 0.07–0.21 m/s (mean velocity = 0.13 ± 0.06 m/s; R^2 values from plots of distance vs. time to determine slope ranged from 0.69 to 0.98). An example is illustrated in Fig. 3c, d. The spread velocity is similar to what has been reported for hippocampus [60].

Slices taken ventral to the principal claustral subregion contain the transitional zone between dorsal claustrum and endopiriform nucleus or principally endopiriform nucleus, and were therefore avoided. It is interesting that slices taken from claustrum dorsal to the cell-dense region showed similar spread extent and spread velocities—in fact, the spatial extent was often greater in these slices because the spatial extent of claustrum was greater. This indicates that the cell-dense region and the more dorsal, less-dense region are functionally similar with regard to intrinsic excitatory connectivity.

Pharmacology of synchronous activity

As bicuculline levels in the slice bath equilibrate, evoked responses increase in amplitude and the early population firing is eventually followed by repetitive spiking (Figs. 3, 4). The number of these late repetitive spikes and their amplitudes both increase during bicuculline equilibration.

Bath application of either high-dose calcium (8 mM) to reduce polysynaptic activity and/or the glutamate receptor antagonist, CNQX, simultaneously eliminate synchronous activity and its spread. High-dose calcium eliminated repetitive population spiking and exposed the typical broadening of propagated population spikes that were smaller, but still all-or-none (Fig. 6). CNQX eliminated responses completely, degrading even the initial population spike and underlying population excitatory postsynaptic potential, until only the stimulus artifact remained (data not shown). Based on these findings, we conclude that the synchronization of cellular activity to support spontaneous population events and their spread are mediated by excitatory glutamatergic synapses.

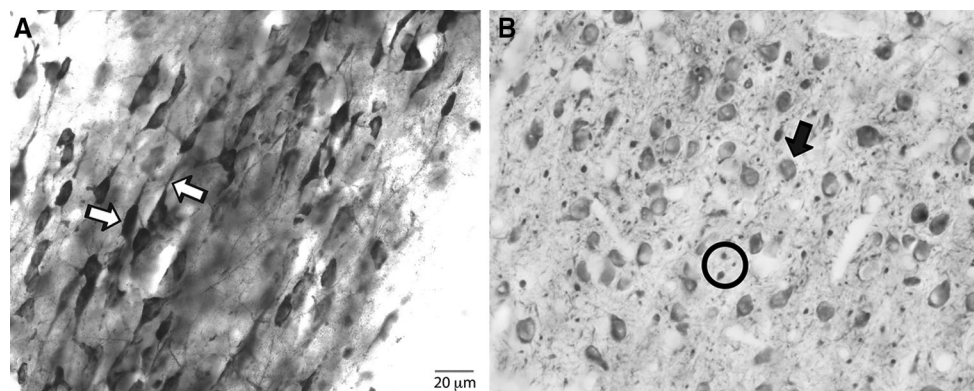


Fig. 2 High-magnification images of latexin-positive claustral cells in sections that capture the dendrites of fusiform cells or cut them in cross-section. Forty-times magnification of latexin staining from an oblique section (**a** comparable to **d** in Fig. 1) and from a coronal section (**b** comparable to **a** in Fig. 1). *White arrows* in (**a**) highlight

fusiform cell bodies and the dendrites of these bipolar neurons. In (**b**), a cross-section of a cell body is marked by a *black arrow* and cross-sections of dendritic elements are highlighted with a *black circle*. *Scale bar* 20 μ m

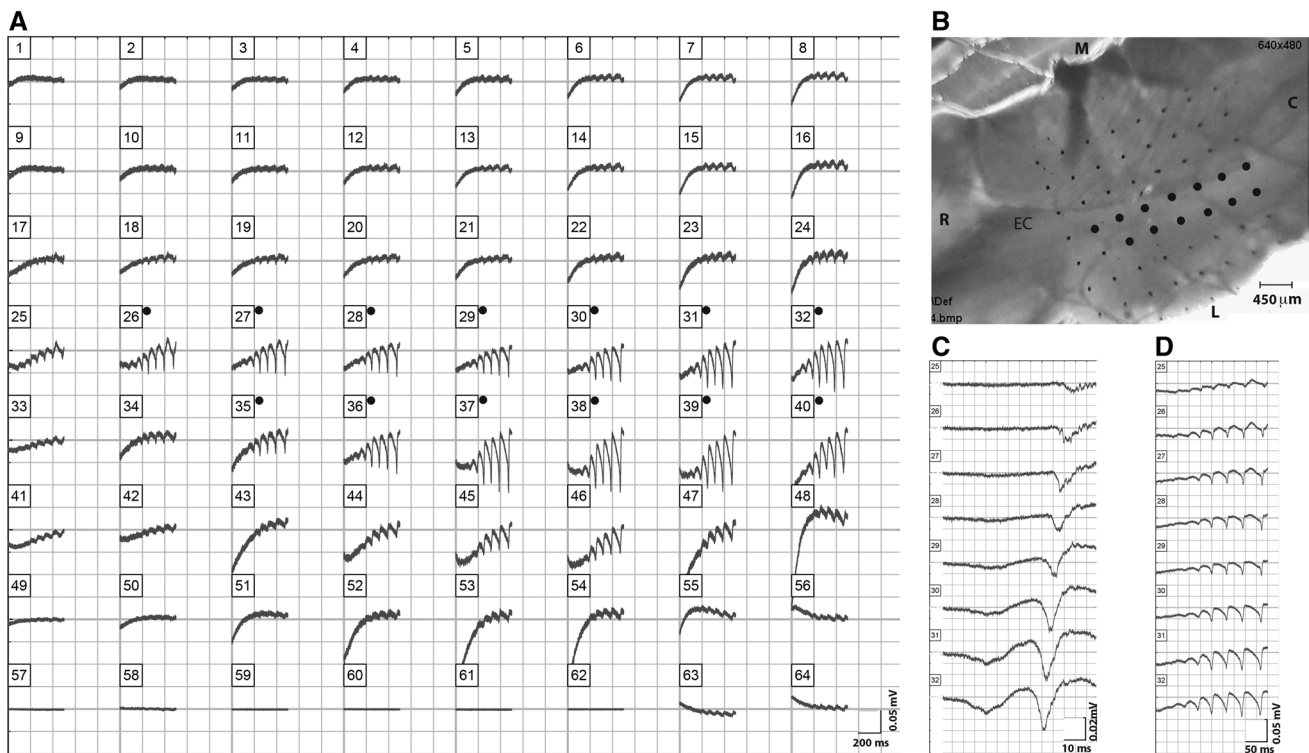


Fig. 3 Spread pattern of spontaneous synchronous population activity in disinhibited oblique slices of claustrum. **a** Multi-channel recording of activity within claustrum and surrounding regions. Although the population activity is confined to claustrum, the activity is present everywhere in claustrum. **b** Image of brain slice and 64 recording channels (*small black dots*). *Large black dots* mark those channels that are within claustrum. *R, C, L, M* indicate rostral, caudal, lateral, and medial borders of the tissue. *EC* indicates external capsule. **c, d** illustrate with higher temporal resolution the spread pattern of a single (initial) spike (**c**) and the later repetitive population spiking (**d**). Details of the degree of claustral involvement in synchronous activity and propagation rates appear in the text. Note the different time calibrations for (**a**), (**c**), and (**d**): 200, 10, and 50 ms per division, respectively

Discussion

Latexin immunohistochemistry and brain slices cut in various planes were used to demonstrate an oblique, rostro-caudally directed organization of bipolar cells, with highly cell-dense and less dense subregions of the rat dorsal claustrum. This intrinsic cellular organization included excitatory cell-to-cell connectivity that, in disinhibited slices, supported the spontaneous generation of synchronized population events that spread along the oblique, rostro-caudal axis. Whereas excitatory connectivity was responsible for synchronous population activity within oblique laminae, segregation of laminar activity was independent of inhibition. These findings suggest modality specificity [31, 32, 61] without cross-talk between modalities.

Significance of dendritic organization and intrinsic connectivity

The directional spread without broadening of activity within claustrum indicates several important features of the intrinsic connectivity. Spread was constrained within the

medial, and lateral borders of the tissue. *EC* indicates external capsule. **c, d** illustrate with higher temporal resolution the spread pattern of a single (initial) spike (**c**) and the later repetitive population spiking (**d**). Details of the degree of claustral involvement in synchronous activity and propagation rates appear in the text. Note the different time calibrations for (**a**), (**c**), and (**d**): 200, 10, and 50 ms per division, respectively

oblique rostro-caudal dimension, and was minimal in coronal and sagittal planes, suggesting preferential modality specific intrinsic communication with minimal interaction across modalities. The absence of broadening indicates that the full network of claustral neurons at each point along the propagation path was being activated [60, 62] (see also Fig. 6), suggesting that the addition of inhibitory circuitry would constrain activity further.

If the claustral sensory modalities are organized in a laminar fashion, as evidenced by Morys, Narkiewicz, and others [31, 32, 61], our data from disinhibited slices suggest that only intra-laminar (within modality interactions), but not inter-laminar (interactions across modalities) interactions occur within claustrum. Inhibitory circuits are expected to refine the intra-laminar connectivity, but are not the basis for inter-laminar segregation. The independence from inhibition for segregation is in contrast to other structures that depend highly on inhibitory circuits to compartmentalize activity (e.g., barrel cortex [63]).

In a review, Crick and Koch [34] discussed claustrum as having a critical role in binding together information from widely separated cortical areas. “A key feature of almost

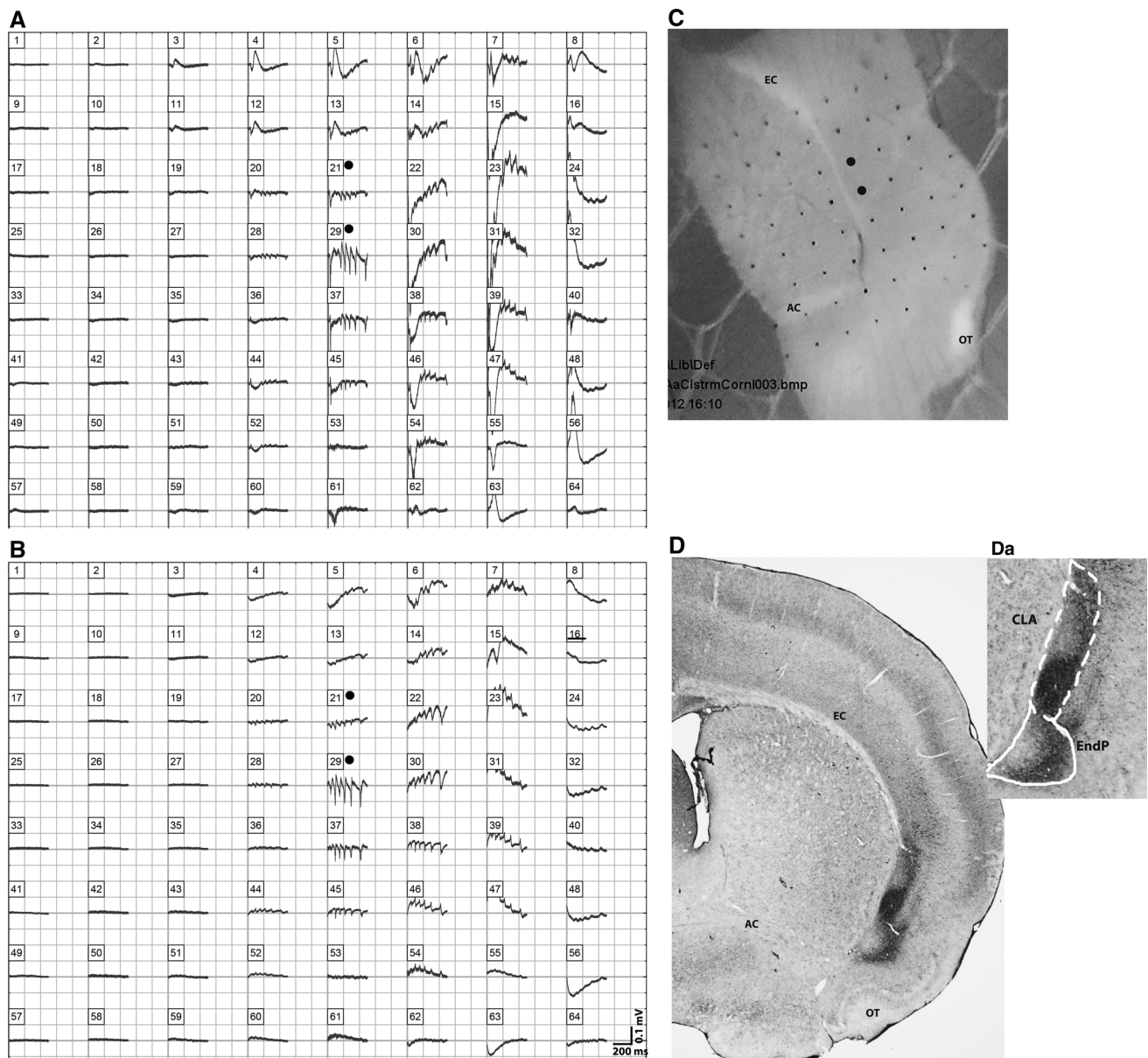


Fig. 4 Failure of spontaneous synchronous population activity spread in disinhibited coronal slices of claustrum. **a** Evoked population discharge in claustrum appears on a single electrode (stimulating electrode poles are visible dorsal to electrodes 7 and 8). **b** Spontaneous synchronous population activity appearing on the same channel. **c** Image of brain slice and 64 recording channels (*small black dots*). *Large black dots* mark those channels that are within the main part of

claustrum. Channel 13 contacts the unstained region, channel 37 contacts a transitional zone between the claustrum and endopiriform nucleus, and channel 45 samples the endopiriform nucleus. **d** Latexin-stained coronal section corresponding to the brain slice shown. *AC* anterior commissure, *EC* external capsule, *OT* optic tract, *CLA* claustrum, and *EndP* endopiriform nucleus. Details of the degree of claustral involvement in synchronous activity appear in the text

all neuronal theories of consciousness is the need for continuous interactions among groups of widely dispersed pyramidal neurons ...” “It is clear that the claustrum lies at the confluence of a large number of simple loops with cortex. This widespread and reciprocal connectivity with many, if not most, cortical regions raises the obvious question: why is all this information brought together?” “... If the claustrum is critical to binding information

within and across sensory and motor modalities ... there must be some sort of intermixing of the associated signals within the claustrum” [34]. The results of this paper suggest that claustrum is well-suited to the broad distribution of activity with a claustral lamina or modality, but that other mechanisms must exist for binding the activity of different laminae or modalities. Clearly, many questions remain unanswered.

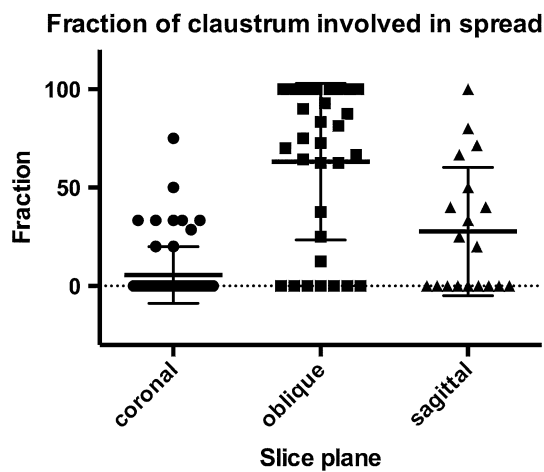


Fig. 5 Differences in the degree of claustral involvement in the spread of synchronous population activity for three planes of section. The fraction of electrodes showing synchronous population activity in relation to the total number of electrodes contacting the latexin-dense claustrum is expressed for coronal, oblique, and sagittal slices. The vast majority of coronal slices showed population activity on 0 or 1 channels, whereas the vast majority of oblique slices showed population activity over nearly 80 % of electrodes. See text for additional details

Latexin binding and claustrum

The original reports of latexin staining by Arimatsu et al. [50, 51, 54–56] were focused on neocortical cell development and specialization. Interestingly, claustrum was clearly well stained and was noted, but not emphasized in any of the reports. Here, we corroborate latexin staining as a useful marker to identify both claustrum and endopiriform nucleus, support subdivisions based on the density of staining, and permit examination of cellular morphology of latexin-positive neurons. The latexin-positive, “egg-shaped” (in coronal sections) claustrum is well-aligned with current anatomical definitions reviewed by Mathur [4].

Potential for seizure generalization and altered consciousness

A central, potentially integrative position held by claustrum is also part of the basis for suggesting a role for claustrum in seizure generalization, and an intra-laminar spread of activity within claustrum could be sufficient for such a role. One of the earliest suggestions for claustrum’s involvement in seizure generation came long before its anatomical relations with neocortex were fully defined. A female epileptic patient was found to have an “enormous” claustrum bilaterally [64].

Claustrum stimulation is efficient for kindling seizure activity [13, 65, 66]. Bilateral claustral lesions impair

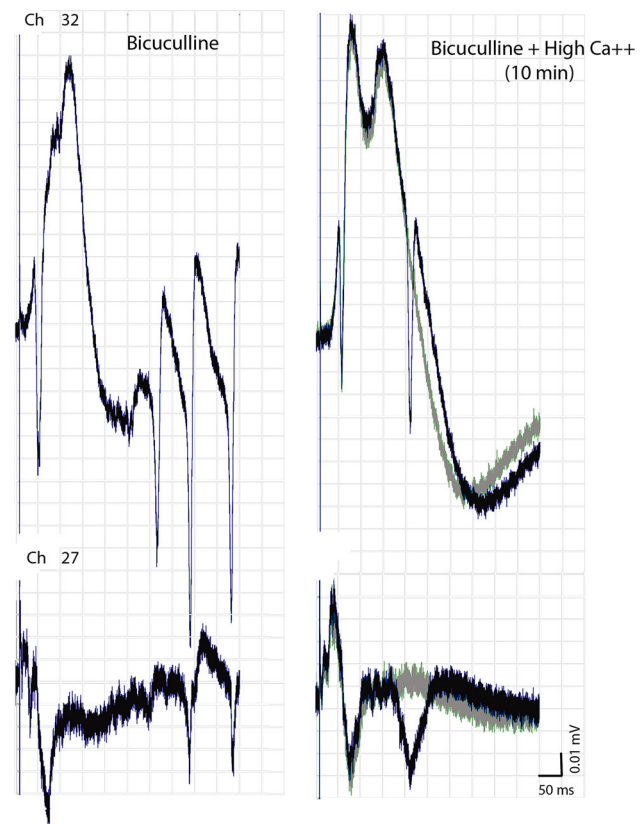


Fig. 6 Failure of population activity after exposure to high calcium-containing media. Two electrodes within an oblique section of claustrum, separated by 2.25 mm (450 μ m interelectrode spacing) showed evoked population bursting that spreads from electrode 32 toward electrode 27. After addition of 8 mM calcium to the ACSF to lower the overall excitability of neurons, population spikes are smaller, less numerous, and the broadening of excitatory–excitatory connections [62] is more readily evident. The all or nothing quality of late population spikes by showing two sweeps superimposed

kindling when stimuli are applied to the amygdala [67], since claustrum sits as a relay structure between amygdala and neocortical regions [68, 69]. Unilateral lesions have complex effects [70, 71] or no effect at all [72]. Seizure activity can be triggered by convulsant application to endopiriform nucleus (ventral claustrum) and prevented by application of glutamate receptor antagonists or GABA to endopiriform nucleus [73–75].

An interesting behavior in endopiriform nucleus neuron studies is the “build-up” of activity in the nucleus before a synchronous epileptiform burst occurs [76, 77], clearly consistent with endopiriform cells exciting one another via their local connectivity [78–80]. In fact, Demir et al. have argued that the circuitry to amplify and sustain excitation is separate from the circuitry that generates the actual epileptiform discharge [81]. Whereas endopiriform can certainly be the origin for synchronized burst discharges,

we find that claustrum is capable of generating such activity completely independently.

A particularly interesting clinical correlate offering potential insights into claustral function is aura [82]. Auras or paroxysmal psychic automatism are experiences characterized by sudden onset, automatic development, vividness, and a clear sense of strangeness to the individual. These are interpreted as partial seizures (reviewed in [83]), a fact reflected in current definitions, for example: “a subjective ictal phenomenon that in a given patient may precede an observable seizure, if alone, constitutes a sensory seizure.” Simple and complex aura experiences have been described, particularly in relation to temporal lobe seizures [84, 85].

Does claustrum cause auras or does claustral activity limit a focal seizure so that only an aura occurs? One possibility is that claustrum becomes overactive and transmits its activity to neocortex or limbic cortex [82]. This means that claustrum must possess the capacity to become overactive on its own, a feature we demonstrate here. Also, activity is expected to spread within a lamina or modality without activation of other modal-specific claustral laminae. The data described in this paper highlight the importance of an intrinsic excitatory glutamatergic network of connections within claustrum, but glutamatergic connections also mediate claustral-cortical and cortico-claustral activity spread. The roles of specific claustral cell types and the contributions of transmitter molecules such as nitric oxide remain poorly understood.

An alternative role for claustrum is that it acts to limit a developing seizure that originates in cortex (i.e., the output of claustrum is inhibitory). Consistent with a regulatory or suppressor role for claustrum are data from SPECT studies of seizure patients with auras, suggesting a “zone of suppression” in cortex during auras [86]. Such a function could be mediated by a direct inhibitory output from claustrum to cortex, excitatory claustral projections whose targets are cortical interneurons, or a local claustral activity change that suppresses activity spread within claustrum itself. Here again, the roles of specific claustral cell types and the contributions of transmitter molecules such as GABA and nitric oxide remain poorly understood.

These are complex questions that will be challenging to address given stimulation and recording limitations imposed by claustrum’s size and shape, and the importance of fully capturing its cells in preparations for physiological study.

Acknowledgments The author is deeply grateful to Dr. Y. Arimatsu for the generous gift of latexin antibodies. Additionally, the author thanks Dr. R.K.S. Wong for critical reading of the manuscript, Dr. R. Kollmar for guidance with microscopy, Dr. F. Scalia for initial guidance on technical aspects of immunohistochemistry, and Ms.

I. Rozenberg for technical assistance. The author expresses her deepest gratitude to Drs. Kiyomi Koizumi and Mark Stewart for their unwavering support. This study was funded in part by support from philanthropic contributions and the University.

Compliance with ethical standards

conflict of interest None.

Research involving human participants and/or animals This research conforms to the standards set forth in the NIH Guide for the Care and Use of Laboratory Animals (8th edn., National Academies Press, 2011) and was approved by the Institutional Animal Care and Use Committee under protocols for the preparation and study of acute brain slices and immunohistochemistry.

Informed consent Not applicable.

References

- Kowianski P, Dziewiatkowski J, Kowianska J, Morys J (1999) Comparative anatomy of the claustrum in selected species: a morphometric analysis. *Brain Behav Evol* 53:44–54
- Sherk H (1986) The claustrum and the cerebral cortex. In: Jones EG, Peters A (eds) *Cerebral cortex* (vol 5) Sensory-motor areas and aspects of cortical connectivity. Plenum, New York, pp. 467–499
- Edelstein LR, Denaro FJ (2004) The claustrum: a historical review of its anatomy, physiology, cytochemistry and functional significance. *Cell Mol Biol* 50:675–702
- Mathur BN (2014) The claustrum in review. *Front Syst Neurosci* 8:48. doi:10.3389/fnsys.2014.00048
- Smythies JR, Edelstein LR, Ramachandran VS (2014) The claustrum: structural, functional, and clinical neuroscience. Academic, San Diego
- Baizer JS, Sherwood CC, Noonan M, Hof PR (2014) Comparative organization of the claustrum: what does structure tell us about function? *Front Syst Neurosci* 8:117. doi:10.3389/fnsys.2014.00117
- Sherk H, LeVay S (1983) Contribution of the cortico-claustral loop to receptive field properties in area 17 of the cat. *J Neurosci* 3:2121–2127
- Carey RG, Neal TL (1985) The rat claustrum: afferent and efferent connections with visual cortex. *Brain Res* 329:185–193. doi:10.1016/0006-8993(85)90524-4
- Kowianski P, Dziewiatkowski J, Berdel B, Lipowska M, Morys J (1998) The cortico-claustral connections in the rat studied by means of the fluorescent retrograde axonal transport method. *Folia Morphol (Warsz)* 57:85–92
- LeVay S (1986) Synaptic organization of claustral and geniculate afferents to the visual cortex of the cat. *J Neurosci* 6:3564–3575
- Kowianski P, Morys J, Dziewiatkowski J, Karwacki Z, Wisniewski HM (2000) The combined retrograde transport and unbiased stereological study of the claustrum-cortical connections in the rabbit. *Ann Anat* 182:111–122
- Druga R (1989) Projections from the claustrum to the occipital cortex in the guinea pig. *Folia Morphol (Praha)* 37:57–63
- Zhang X, Hannelson DK, Saucier DM, Wallace AE, Howland J, Corcoran ME (2001) Susceptibility to kindling and neuronal connections of the anterior claustrum. *J Neurosci* 21:3674–3687
- Druga R (1982) Claustral-neocortical connections in the cat and rat demonstrated by HRP tracing technique. *J Hirnforsch* 23:191–202

15. Kowianski P, Morys J, Sadowski M, Dziewiatkowski J (2000) Qualitative and quantitative differences in the motor and somatosensory cortical projections of the rat claustrum—combined retrograde transport and stereological studies. *Folia Morphol (Warsz)* 59:111–119
16. Druga R (1966) Cortico-claustral connections. I. Fronto-claustral connections. *Folia Morphol (Praha)* 14:391–399
17. Druga R (1968) Cortico-claustral connections. II. Connections from the parietal, temporal and occipital cortex to the claustrum. *Folia Morphol (Praha)* 16:142–149
18. Beneyto M, Prieto JJ (2001) Connections of the auditory cortex with the claustrum and the endopiriform nucleus in the cat. *Brain Res Bull* 54:485–498. doi:10.1016/S0361-9230(00)00454-8
19. Fu W, Sugai T, Yoshimura H (2004) Onoda N (2004) Convergence of olfactory and gustatory connections onto the endopiriform nucleus in the rat. *Neuroscience* 126:1033–1041. doi:10.1016/j.neuroscience.03.041S0306452204002374
20. Chachich ME (2004) Powell DA (2004) The role of claustrum in Pavlovian heart rate conditioning in the rabbit (*Oryctolagus cuniculus*): anatomical, electrophysiological, and lesion studies. *Behav Neurosci* 118:514–525. doi:10.1037/0735-7044.118.3.514-95232-008
21. Majak K, Kowianski P, Morys J, Spodnik J, Karwacki Z, Wisniewski HM (2000) The limbic zone of the rabbit and rat claustrum: a study of the claustrorostriate connections based on the retrograde axonal transport of fluorescent tracers. *Anat Embryol (Berl)* 201:15–25
22. Majak K, Kowianski P, Dziewiatkowski J, Karwacki Z, Luczynska A, Morys J (2000) Claustrorostriate connections in the rabbit and rat—a stereological study. *Folia Morphol (Warsz)* 59:47–56
23. Markowitsch HJ, Irle E, Bang-Olsen R, Flindt-Egebak P (1984) Claustral efferents to the cat's limbic cortex studied with retrograde and anterograde tracing techniques. *Neuroscience* 12:409–425. doi:10.1016/0306-4522(84)90062-9
24. Wilhite BL, Teyler TJ, Hendricks C (1986) Functional relations of the rodent claustral-entorhinal-hippocampal system. *Brain Res* 365:54–60. doi:10.1016/0006-8993(86)90721-3
25. Eid T, Jorritsma-Byham B, Schwarcz R, Witter MP (1996) Afferents to the seizure-sensitive neurons in layer III of the medial entorhinal area: a tracing study in the rat. *Exp Brain Res* 109:209–218
26. Macchi G, Bentivoglio M, Minciacchi D, Molinari M (1981) The organization of the claustroneocortical projections in the cat studied by means of the HRP retrograde axonal transport. *J Comp Neurol* 195:681–695. doi:10.1002/cne.901950411
27. Olson CR, Graybiel AM (1980) Sensory maps in the claustrum of the cat. *Nature* 288:479–481
28. Fernandez-Miranda JC, Rhoton AL Jr, Kakizawa Y, Choi C, Alvarez-Linera J (2008) The claustrum and its projection system in the human brain: a microsurgical and tractographic anatomical study. *J Neurosurg* 108:764–774. doi:10.3171/JNS/2008/108/4/0764
29. Narkiewicz O (1964) Degenerations in the Claustrum after Regional Neocortical Ablations in the Cat. *J Comp Neurol* 123:335–355
30. Druga R (1971) Projection of prepyriform cortex into claustrum. *Folia Morphol (Praha)* 19:405–410
31. Kowianski P, Morys J, Karwacki Z, Dziewiatkowski J, Narkiewicz O (1998) The cortico-related zones of the rabbit claustrum—study of the claustrorostriate connections based on the retrograde axonal transport of fluorescent tracers. *Brain Res* 784:199–209. doi:10.1016/S0006-8993(97)01326-7
32. Sadowski M, Morys J, Jakubowska-Sadowska K, Narkiewicz O (1997) Rat's claustrum shows two main cortico-related zones. *Brain Res* 756:147–152. doi:10.1016/S0006-8993(97)00135-2
33. Sloniewski P, Usunoff KG, Pilgrim C (1986) Retrograde transport of fluorescent tracers reveals extensive ipsi- and contralateral claustrorostriate connections in the rat. *J Comp Neurol* 246:467–477. doi:10.1002/cne.902460405
34. Crick FC, Koch C (2005) What is the function of the claustrum? *Philos Trans R Soc Lond B* 360:1271–1279. doi:10.1098/rstb.2005.1661
35. Smith JB, Alloway KD (2014) Interhemispheric claustral circuits coordinate sensory and motor cortical areas that regulate exploratory behaviors. *Front Syst Neurosci* 8:93. doi:10.3389/fnsys.2014.00093
36. Perez-Cerda F, Martinez-Millan L, Matute C (1996) Anatomical evidence for glutamate and/or aspartate as neurotransmitters in the geniculo-, claustrorostriate-, and cortico-cortical pathways to the cat striate cortex. *J Comp Neurol* 373:422–432. doi:10.1002/(SICI)1096
37. Cudeiro J, Rivadulla C, Rodriguez R, Grieve KL, Martinez-Conde S, Acuna C (1997) Actions of compounds manipulating the nitric oxide system in the cat primary visual cortex. *J Physiol* 504(Pt 2):467–478
38. Narkiewicz O, Nitecka L, Mamos L, Morys J (1988) The pattern of the GABA-like immunoreactivity in the claustrum. *Folia Morphol (Warsz)* 47:21–30
39. Kowianski P, Timmermans JP, Morys J (2001) Differentiation in the immunocytochemical features of intrinsic and cortically projecting neurons in the rat claustrum – combined immunocytochemical and axonal transport study. *Brain Res* 905:63–71. doi:10.1016/S0006-8993(01)02408-8
40. Mamos L (1984) Morphology of claustral neurons in the rat. *Folia Morphol (Warsz)* 43:73–78
41. Mamos L, Narkiewicz O, Morys J (1986) Neurons of the claustrum in the cat; a Golgi study. *Acta Neurobiol Exp (Wars)* 46:171–178
42. Wasilewska B, Najdzion J (2001) Types of neurons of the claustrum in the rabbit—Nissl, Kluver-Barrera and Golgi studies. *Folia Morphol (Warsz)* 60:41–45
43. Rahman FE, Baizer JS (2007) Neurochemically defined cell types in the claustrum of the cat. *Brain Res* 1159:94–111. doi:10.1016/j.brainres.2007.05.011
44. Gomez-Urquijo SM, Gutierrez-Ibarluzea I, Bueno-Lopez JL, Reblet C (2000) Percentage incidence of gamma-aminobutyric acid neurons in the claustrum of the rabbit and comparison with the cortex and putamen. *Neurosci Lett* 282:177–180
45. Wojcik S, Dziewiatkowski J, Spodnik E, Ludkiewicz B, Domaradzka-Pytel B, Kowianski P, Morys J (2004) Analysis of calcium binding protein immunoreactivity in the claustrum and the endopiriform nucleus of the rabbit. *Acta Neurobiol Exp (Wars)* 64:449–460
46. Davila JC, Real MA, Olmos L, Legaz I, Medina L, Guirado S (2005) Embryonic and postnatal development of GABA, calbindin, calretinin, and parvalbumin in the mouse claustral complex. *J Comp Neurol* 481:42–57. doi:10.1002/cne.20347
47. Obst-Pernberg K, Medina L, Redies C (2001) Expression of R-cadherin and N-cadherin by cell groups and fiber tracts in the developing mouse forebrain: relation to the formation of functional circuits. *Neuroscience* 106:505–533. doi:10.1016/S0306-4522(01)00292-5
48. Korematsu K, Redies C (1997) Restricted expression of cadherin-8 in segmental and functional subdivisions of the embryonic mouse brain. *Dev Dyn* 208:178–189. doi:10.1002/(SICI)1097
49. Real MA, Davila JC, Guirado S (2003) Expression of calcium-binding proteins in the mouse claustrum. *J Chem Neuroanat* 25:151–160
50. Arimatsu Y, Ishida M (1998) Early patterning of the rat cerebral wall for regional organization of a neuronal population expressing latexin. *Brain Res Dev Brain Res* 106:71–78

51. Arimatsu Y, Nihonmatsu I, Hatanaka Y (2009) Localization of latexin-immunoreactive neurons in the adult cat cerebral cortex and claustrum/endopiriform formation. *Neuroscience* 162:1398–1410. doi:[10.1016/j.neuroscience.2009.05.060](https://doi.org/10.1016/j.neuroscience.2009.05.060)
52. Orman R, Patel K, Scalia F (2011) The rat claustrum: anatomical axes defined by cellular morphology. Eighth IBRO World Congress of Neuroscience. Italy, Florence, p C254
53. Orman R (2009) Intrinsic connectivity of claustrum. XXXVI International Congress of Physiological Sciences (IUPS2009). Journal of Physiological Sciences, Kyoto, Japan, pp P2PM-11-15
54. Arimatsu Y (1994) Latexin: a molecular marker for regional specification in the neocortex. *Neurosci Res* 20:131–135
55. Arimatsu Y, Ishida M, Sato M, Kojima M (1999) Corticocortical associative neurons expressing latexin: specific cortical connectivity formed in vivo and in vitro. *Cereb Cortex* 9:569–576
56. Arimatsu Y, Miyamoto M, Nihonmatsu I, Hirata K, Uratani Y, Hatanaka Y, Takiguchi-Hayashi K (1992) Early regional specification for a molecular neuronal phenotype in the rat neocortex. *Proc Natl Acad Sci USA* 89:8879–8883
57. Paxinos G, Watson C (1998) The rat brain in stereotaxic coordinates, 4th edn. Academic, San Diego
58. Paxinos G, Watson C (2007) The rat brain in stereotaxic coordinates, 6th edn. Academic, Boston
59. Mathur BN, Caprioli RM, Deutch AY (2009) Proteomic analysis illuminates a novel structural definition of the claustrum and insula. *Cereb Cortex* 19:2372–2379. doi:[10.1093/cercor/bhn253](https://doi.org/10.1093/cercor/bhn253)
60. Orman R, Von Gizycki H, Lytton WW, Stewart M (2008) Local axon collaterals of area CA1 support spread of epileptiform discharges with CA1, but propagation is unidirectional. *Hippocampus* 18:1021–1033. doi:[10.1002/hipo.20460](https://doi.org/10.1002/hipo.20460)
61. Jakubowska-Sadowska K, Morys J, Sadowski M, Kowianski P, Karwacki Z, Narkiewicz O (1998) Visual zone of the claustrum shows localization and organizational differences among rat, guinea pig, rabbit and cat. *Anat Embryol (Berl)* 198:63–72
62. Lytton WW, Orman R, Stewart M (2008) Broadening of activity with flow across neural structures. *Perception* 37:401–407
63. Sun QQ, Huguenard JR, Prince DA (2006) Barrel cortex microcircuits: thalamocortical feedforward inhibition in spiny stellate cells is mediated by a small number of fast-spiking interneurons. *J Neurosci* 26:1219–1230. doi:[10.1523/JNEUROSCI.4727-04.2006](https://doi.org/10.1523/JNEUROSCI.4727-04.2006)
64. Fawcett E (1894) Anatomical notes. I. Brain with an enormously enlarged claustrum. *J Anat Physiol* 28:116–118
65. Sheerin AH, Nysten K, Zhang X, Saucier DM, Corcoran ME (2004) Further evidence for a role of the anterior claustrum in epileptogenesis. *Neuroscience* 125:57–62. doi:[10.1016/j.neuroscience.2004.01.043S0306452204000600](https://doi.org/10.1016/j.neuroscience.2004.01.043S0306452204000600)
66. Mohapel P, Zhang X, Gillespie GW, Chlan-Fourney J, Hannesson DK, Corley SM, Li XM, Corcoran ME (2001) Kindling of claustrum and insular cortex: comparison to perirhinal cortex in the rat. *Eur J Neurosci* 13:1501–1519
67. Mohapel P, Hannesson DK, Armitage LL, Gillespie GW, Corcoran ME (2000) Claustral lesions delay amygdaloid kindling in the rat. *Epilepsia* 41:1095–1101
68. Wada JA, Tsuchimochi H (1997) Role of the claustrum in convulsive evolution of visual afferent and partial nonconvulsive seizure in primates. *Epilepsia* 38:897–906
69. Majak K, Pikkarainen M, Kempainen S, Jolkkonen E, Pitkanen A (2002) Projections from the amygdaloid complex to the claustrum and the endopiriform nucleus: a Phaseolus vulgaris leucoagglutinin study in the rat. *J Comp Neurol* 451:236–249. doi:[10.1002/cne.10346](https://doi.org/10.1002/cne.10346)
70. Morys J, Sloniewski P, Narkiewicz O (1988) Somatosensory evoked potentials following lesions of the claustrum. *Acta Physiol Pol* 39:475–483
71. Wada JA, Kudo T (1997) Involvement of the claustrum in the convulsive evolution of temporal limbic seizure in feline amygdaloid kindling. *Electroencephalogr Clin Neurophysiol* 103:249–256
72. Kudo T, Wada JA (1990) The effect of unilateral claustral lesion on intermittent light stimulation induced seizure in D, L-allyl-glycine treated cats. *Jpn J Psychiatry Neurol* 44:436–437
73. Piredda S, Gale K (1985) A crucial epileptogenic site in the deep prepiriform cortex. *Nature* 317:623–625
74. Piredda S, Pavlick M, Gale K (1987) Anticonvulsant effects of GABA elevation in the deep prepiriform cortex. *Epilepsy Res* 1:102–106
75. Piredda S, Gale K (1986) Role of excitatory amino acid transmission in the genesis of seizures elicited from the deep prepiriform cortex. *Brain Res* 377:205–210. doi:[10.1016/0006-8993\(86\)90859-0](https://doi.org/10.1016/0006-8993(86)90859-0)
76. Hoffman WH, Haberly LB (1993) Role of synaptic excitation in the generation of bursting-induced epileptiform potentials in the endopiriform nucleus and piriform cortex. *J Neurophysiol* 70:2550–2561
77. Hoffman WH, Haberly LB (1996) Kindling-induced epileptiform potentials in piriform cortex slices originate in the underlying endopiriform nucleus. *J Neurophysiol* 76:1430–1438
78. Demir R, Haberly LB, Jackson MB (2001) Epileptiform discharges with in vivo-like features in slices of rat piriform cortex with longitudinal association fibers. *J Neurophysiol* 86:2445–2460
79. Hoffman WH, Haberly LB (1989) Bursting induces persistent all-or-none EPSPs by an NMDA-dependent process in piriform cortex. *J Neurosci* 9:206–215
80. Hoffman WH, Haberly LB (1991) Bursting-induced epileptiform EPSPs in slices of piriform cortex are generated by deep cells. *J Neurosci* 11:2021–2031
81. Demir R, Haberly LB, Jackson MB (1999) Sustained and accelerating activity at two discrete sites generate epileptiform discharges in slices of piriform cortex. *J Neurosci* 19:1294–1306
82. Sperner J, Sander B, Lau S, Krude H, Scheffner D (1996) Severe transitory encephalopathy with reversible lesions of the claustrum. *Pediatr Radiol* 26:769–771
83. Alvarez-Silva S, Alvarez-Silva I, Alvarez-Rodriguez J, Perez-Echeverria MJ, Campayo-Martinez A, Rodriguez-Fernandez FL (2006) Epileptic consciousness: concept and meaning of aura. *Epilepsy Behav* 8:527–533. doi:[10.1016/j.yebeh.2005.12.013](https://doi.org/10.1016/j.yebeh.2005.12.013)
84. Taylor DC, Lochery M (1987) Temporal lobe epilepsy: origin and significance of simple and complex auras. *J Neurol Neurosurg Psychiatry* 50:673–681
85. Kanemoto K, Janz D (1989) The temporal sequence of aura-sensations in patients with complex focal seizures with particular attention to ictal aphasia. *J Neurol Neurosurg Psychiatry* 52:52–56
86. Ramsay SC, McLaughlin AF, Greenough R, Walsh J, Morris JG (1992) Comparison of independent aura, ictal and interictal cerebral perfusion. *J Nucl Med* 33:438–440